Bio-Medical Materials and Engineering 20 (2010) 89–97
DOI 10.3233/BME-2010-0618
IOS Press

A practical biomechanical model of the index finger simulating the kinematics of the muscle/tendon excursions

John Z. Wu [a,*], Kai-Nan An [b], Robert G. Cutlip [a] and Ren G. Dong [a]
[a] *National Institute for Occupational Safety and Health, Morgantown, WV, USA*
[b] *Mayo Clinic, Rochester, MN, USA*

Received 4 July 2008
Accepted 25 February 2010

Abstract. Biomechanical models of the hand and fingers are useful tools for hand surgeons to improve surgical procedures and for biomedical researchers to explore the mechanical loading in the musculoskeletal system that cannot be easily measured *in vivo*. The purpose of the present study was to develop a realistic index finger model for solving practical problems. The model includes the meshes of four bony sections (distal, middle, proximal and metacarpal bones) obtained via micro-CT scans. The tendon attachment sites are adopted from the normative finger model. A total of seven tendon/muscles are included in the model. The predicted tendon excursions and moment arms were compared with published experimental data. One of the advantages of the current approach over previous studies is that the current model has been developed on a platform of a commercial software package, such that researchers can apply it as a universal tool for practical problems.

Keywords: Index finger, kinematics, muscle–tendon excursion, moment arm, simulations

1. Introduction

There are multiple biomechanical models of the hand and fingers simulating different problems. For example, Sancho-Bru et al. [1] developed a whole hand model simulating the muscle loading for static gripping and free movements; Brook et al. [2] developed a biomechanical model of the dynamics of the index finger and applied their model to simulate the muscle forces in pinch grip and disc rotation; Biggs and Horch [3] proposed a 3D kinematic long finger model and qualitatively validated their model via the experimental data of tendon/muscle excursions for the motion of the MCP joint. The biomechanical finger models proposed by Valero-Cuevas et al. [4] included anatomically realistic tendon/muscle connections and musculoskeletal parameters. All these mathematical hand models are formulated analytically and rely on certain simplifying assumptions.

The theories of the tendon excursion and muscle moment arm for the finger, which researchers apply today, are based on three Landsmeer's models [5,6] and the normative model [7]. The relationships between the moment arm, excursion, and joint angle are formulated mathematically in these models. According to the classical theory, the instantaneous moment arm of a tendon with respect to the axis of

* Address for correspondence: John Z. Wu, PhD, NIOSH/CDC, 1095 Willowdale Road, MS-2027, Morgantown, WV 26505, USA. Tel.: +1 304 285-5832; Fax: +1 304 285-6265; E-mail: jwu@cdc.gov.

0959-2989/10/$27.50 © 2010 – IOS Press and the authors. All rights reserved

a joint movement is the slope of the tendon excursion with respect to the corresponding joint rotation. Using these theories, An et al. [8] experimentally determined the tendon excursion and moment arm of the fingers. In their tests, the tendon excursions were measured directly using displacement transducers while the moment arms were derived from the excursion data. Fowler et al. [9] determined the moment arms and lines of action of the tendons in the index finger using a direct optical measurement from the high resolution MRI scans. The results obtained using these two different approaches have not been compared. In the current study, we developed a simulation of joint kinematics and muscle/tendon excursions to predict the index finger moment arms by using the commercial software AnyBody (version 2.0, AnyBody Technology, Aalborg, Denmark). The model predictions are compared with published experimental data.

2. Methods

The index finger is modeled as a linkage system, based on the normative model [7], as illustrated in Fig. 1. The index finger consists of distal, middle, proximal phalanges, and metacarpal bones. The DIP (distal interphalangeal) and PIP (proximal interphalangeal) joints are modeled as hinges with one DOF in the z-axis; while the MCP (metacarpophalangeal) joint is modeled as a universal joint with two DOFs in the y- and z-axes. The centers of the DIP, PIP and MCP are considered to be located at O_2, O_4 and O_6, respectively, as shown in Fig. 1. The attachment locations of the tendons are defined according to the normative model (Fig. 1). Seven muscles were included in the proposed model: Flexor profundus (FP), flexor sublimis (FS), extensor indicis (EI), extensor digitorum communis (EC), radial interosseous (RI), ulnar interosseous (UI) and lumbrical (LU).

In order to visualize the muscle/tendon attachment locations and to guide the muscle/tendon during the movements, the real bony section meshes were implemented into the proposed index finger model, as shown in Fig. 2(a). These bony section meshes were obtained via CT scanning of a cadaver right hand and input in a STL-format. The lengths of each bony section scan have been scaled to fit to the required phalanx lengths in the index finger model. Since the bony meshes are not recognized as "contact surfaces" in AnyBody, we built ellipsoids at the bony contact ends to guide the muscles/tendons. The muscle/tendons slide on the surfaces of the ellipsoids which mimic the bony surfaces. Figure 2(b, c) depicts the muscle/tendon paths as they wrap on the ellipsoidal models for the bony surfaces at the PIP and DIP joints.

In order to calibrate and validate the proposed model, the predicted muscle/tendon excursions and moment arms were compared with the experimental data by Fowler et al. [9] and An et al. [8]. Since the finger dimensions are normalized in our model, we have to scale the model back to the real finger dimensions to make our results comparable with the published experimental data. The dimensions of the index finger model are scaled by the following factor:

$$\textit{Middle Phalanx Length Scale}\,(O_2O_3) = \frac{\textit{Middle phalanx length} + \textit{DIP joint depth}}{O_1O_2 + O_2O_3}, \tag{1}$$

where *Middle phalanx length* and *DIP joint depth* of the index finger are 21.3 and 4.2 mm, respectively, adopted from [9]; O_1O_2 and O_2O_3 are the normalized DIP joint depth and middle phalanx length defined in the normative model [7], as shown in Fig. 1.

After scaling our finger model to the dimensions in the experiments [9], while maintaining the scaling proportion of the normative finger model, the model predictions are comparable to the experimen-

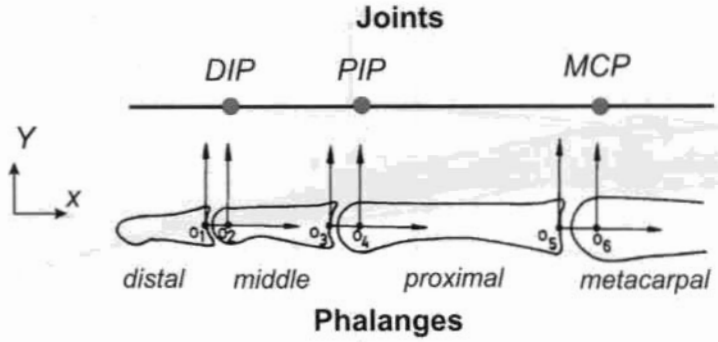

O1 O2	O2 O3	O3 O4	O4 O5	O5 O6
0.228	1.000	0.288	1.919	0.432

		Distal Point				Proximal Point			
Joint	Tendon	X	Y	Z	ΔR	X	Y	Z	ΔR
IP	EC/EI	0.026 (0.004)	0.169 (0.199)	-0.010 (-0.010)	0.037	0.050 (0.000)	0.100 (0.196)	-0.009 (-0.009)	0.108
	FP	0.010 (0.004)	-0.184 (-0.184)	0.026 (0.026)	0.006	0.150 (0.300)	-0.200 (-0.245)	0.054 (0.054)	0.157
MP	FP	-0.212 (-0.212)	-0.308 (-0.308)	0.009 (0.009)	0.000	0.450 (0.400)	-0.209 (-0.409)	0.027 (0.027)	0.206
	RI	-0.112 (-0.112)	0.186 (0.186)	0.223 (0.223)	0.000	0.100 (0.100)	0.200 (0.181)	0.268 (0.268)	0.019
	UI	-0.112 (-0.112)	0.151 (0.151)	-0.290 (-0.290)	0.000	0.100 (0.100)	0.191 (0.131)	-0.312 (-0.312)	0.060
	FS	-0.212 (-0.212)	-0.249 (-0.249)	0.015 (0.015)	0.000	0.400 (0.400)	-0.211 (-0.311)	0.028 (0.028)	0.100
	EC/EI	-0.038 (-0.038)	0.278 (0.278)	-0.027 (-0.027)	0.000	0.050 (0.000)	0.200 (0.266)	-0.026 (-0.026)	0.083
CMC	FP	-0.218 (-0.118)	-0.386 (-0.386)	0.031 (0.031)	0.100	0.450 (0.300)	-0.459 (-0.619)	-0.150 (0.004)	0.266
	FS	-0.218 (-0.118)	-0.477 (-0.477)	-0.074 (-0.074)	0.100	0.550 (0.300)	-0.489 (-0.689)	-0.114 (-0.114)	0.320
	RI	-0.318 (-0.318)	-0.033 (-0.033)	0.443 (0.443)	0.000	0.300 (0.400)	-0.362 (-0.362)	0.529 (0.629)	0.141
	LU	-0.318 (-0.318)	-0.148 (-0.148)	0.370 (0.370)	0.000	0.400 (0.400)	-0.650 (-0.704)	0.200 (0.541)	0.345
	UI	-0.318 (-0.318)	-0.039 (-0.039)	-0.461 (-0.461)	0.000	0.400 (0.400)	-0.279 (-0.379)	-0.242 (-0.442)	0.224
	EC/EI	-0.018 (-0.018)	0.421 (0.421)	-0.033 (-0.033)	0.000	0.000 (0.000)	0.483 (0.483)	-0.026 (-0.026)	0.000

Fig. 1. Schematics of the proposed finger model and tendon attachment locations. O_1, O_2, O_3, O_4, O_5 and O_6 are characteristic markers. The DIP, PIP and MCP joints are assumed to be located at O_2, O_4 and O_6, respectively. The finger dimensions and tendon attachment locations are normalized to the length of the middle phalange, O_2O_3. The locations of the tendon attachment used in the current simulations are compared with those of normative model [7] (numbers in parentheses). ΔR is the adjustment distance of the attachment locations in the current model from the original normative model [7].

tal data. We only calculated the excursions of each individual muscle/tendon; the moment arm of the muscles/tendons corresponding to a particular joint is derived by differentiating of the excursions with respect to that joint rotation. In the numerical tests, the variations of the muscle/tendon excursion and moment arm in response to the flexion/extension of the DIP and PIP joints as well as the flexion/extension and adduction/abduction of the MCP joint individually are calculated and compared with the experimental data.

3. Results

The model predictions of the moment arm of the muscle/tendon corresponding to the MCP abduction(−)/adduction(+) and extension(−)/flexion(+) are shown in Fig. 3(a) and (b), respectively. It is seen that the model predictions agree in trend with the experimental data [9]. In the MCP exten-

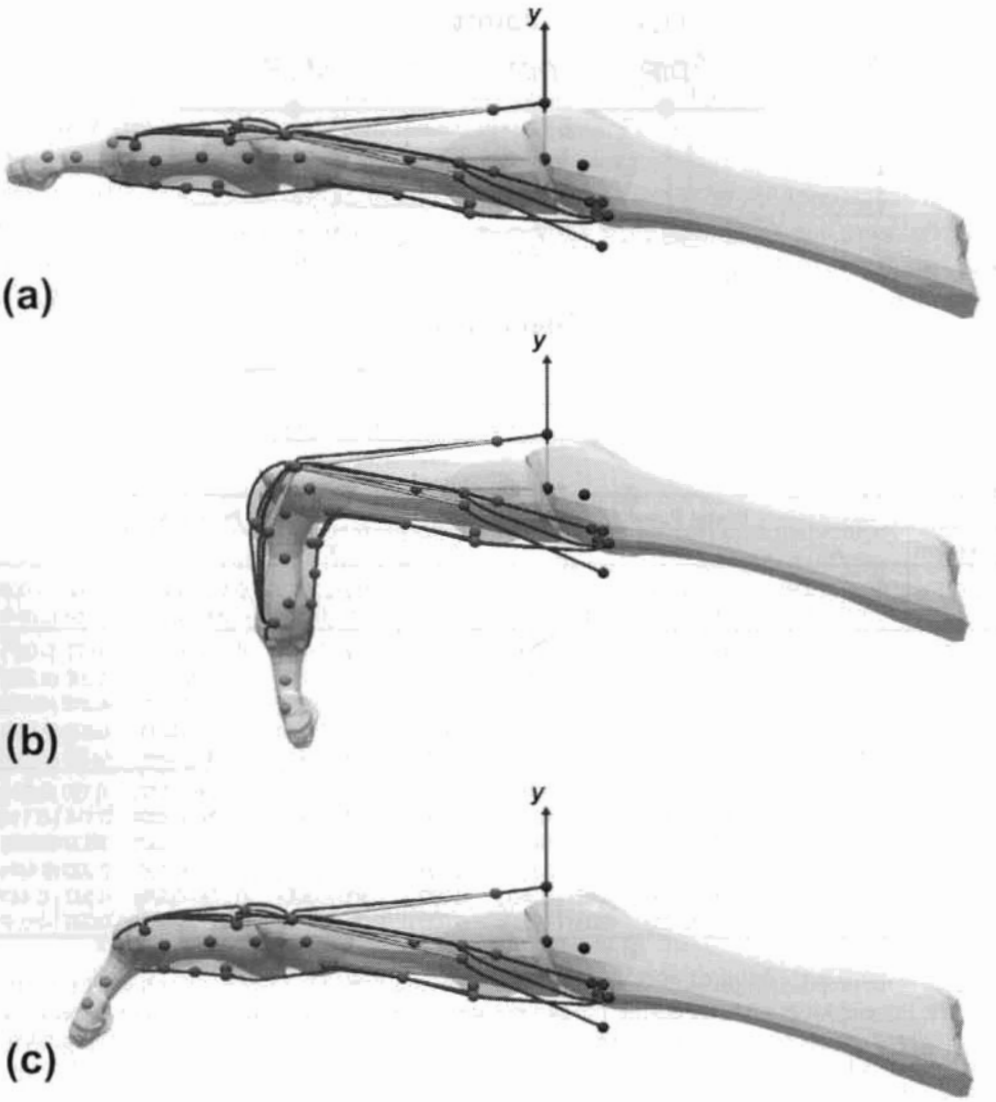

Fig. 2. Schematics of the proposed finger model. (a) Straight position. (b) PIP joint flexed by 90°. (c) DIP joint flexed by 60°. The figures show that the muscles wrap over the bony surfaces and confined by the pulleys.

sion/flexion test (Fig. 3(a)), both model predictions and experimental data indicated that the moment arms for the EI/EC muscles are positive and they are distributed in a narrow range; while those for the RI/UI/LU/FS/FP muscles are negative and spread in a greater range. In the MCP adduction/abduction test (Fig. 3(b)), the model predictions agree in trend with the experimental data (the UI and RI muscles have the maximal positive and negative moment arms, respectively, and the moment arms of all other muscles fall within a range between them). The predicted moment arms of the muscles/tendons corresponding to the PIP flexion are compared with the experimental data in Fig. 3(c). Since the moment arms of EI and EC muscles are identical, only the result for the EI muscle is shown (Fig. 3(c)). The model predictions agree in trend with the experimental measurements (as shown in Fig. 3(c)). For the test with DIP joint extension/flexion, there are only three relevant muscles (Fig. 3(d)), in which the excursion of

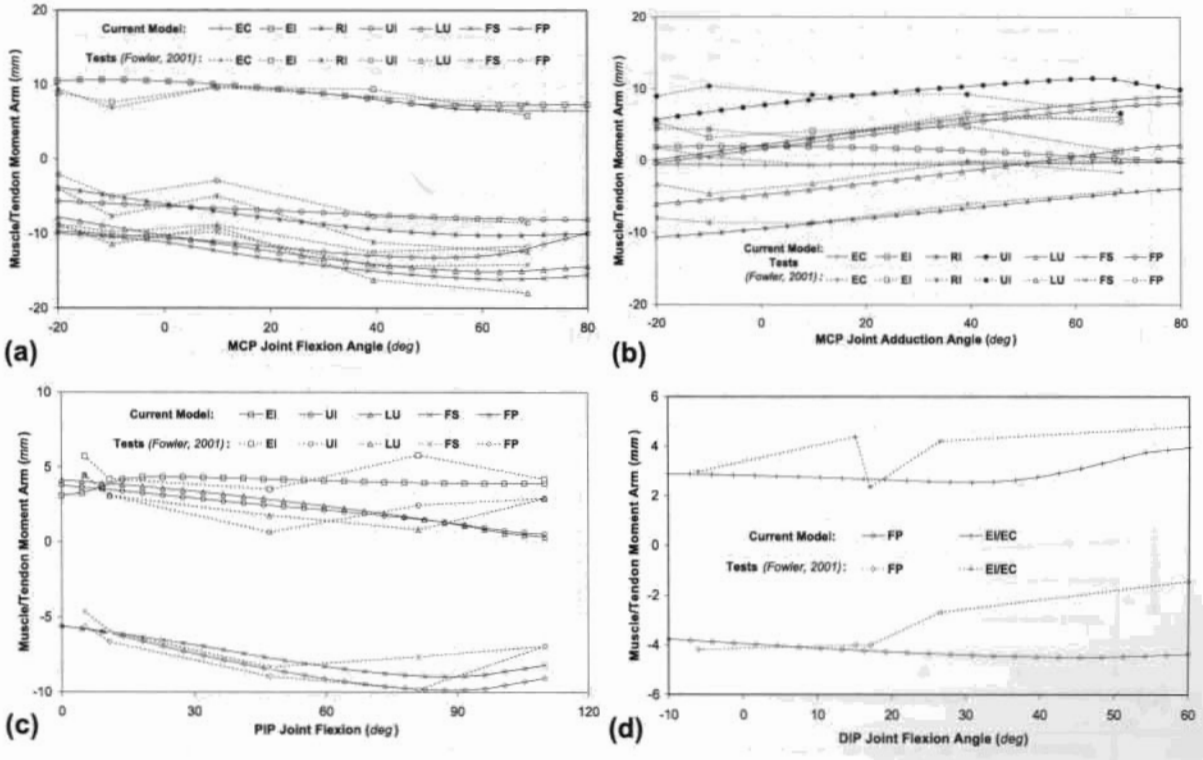

Fig. 3. The predicted muscle/tendon moment arms as a function of the joint motion compared with the corresponding experimental data [9]. (a and b) MCP joint flexion and adduction, respectively. (c) PIP joint flexion. (d) DIP joint flexion.

the EI/EC muscles are identical. Again, the predicted moment arms of the muscle/tendon agree well with the experimental data in trends.

Using the same tendon attachment locations and finger dimensions, the muscle excursions and moment arms corresponding to the experiments [8] have been predicted and compared with their measurements (Fig. 4). The predicted muscle excursions and moment arms for the MC joint extension are compared with those measured experimentally [8] in Fig. 4(a) and (b). It is seen that the predicted excursions and moment arms for RI, UI and LU muscles are greater than the experimental data, while the model predictions agree well with the experimental data for the four muscles (i.e., FP, FS, EI and EC). The comparison between the model predictions and experimental data for the excursion and moment arm corresponding to the MC joint adduction is illustrated in Fig. 4(c) and (d). The predicted muscle excursion and moment arms are consistent with the experimental measurements except for the RI and UI muscles, in which the predicted excursion and moment arm are considerably greater than the experimental data. The predicted muscle excursions and moment arms corresponding to the PIP joint flexion agree closely with the experimental data [7] for all six relevant muscles (EC, EI, UI, LU, FS, and FP), as depicted in Fig. 4(e) and (f), respectively. In this case, An et al. [8] provided only the average moment arms, which have been plotted as a constant and compared with the model predictions in Fig. 4(f). For the case of DIP joint flexion (Fig. 4(g) and (h)), the predicted muscle excursions and moment arms for the FP muscle also agree closely with the experimental measurement [8], while the model predictions and experimental data differ slightly for the EC/EI muscles.

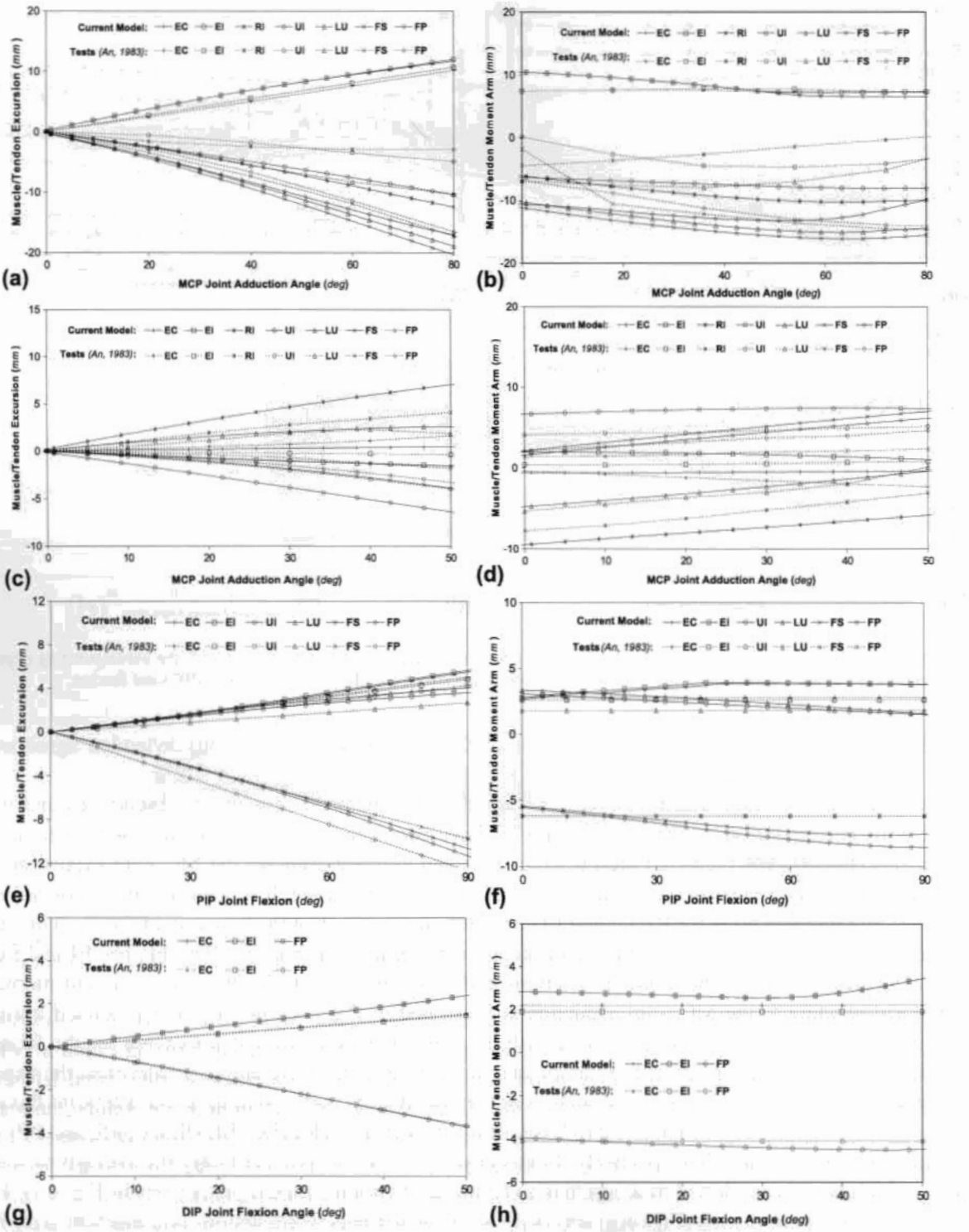

Fig. 4. The predicted muscle/tendon excursions and moment arms as a function joint motions compared with the corresponding experimental data [8]. Left column ((a), (c), (e) and (g)): muscle/tendon excursions. Right column ((b), (d), (f) and (h)): muscle/tendon moment arms.

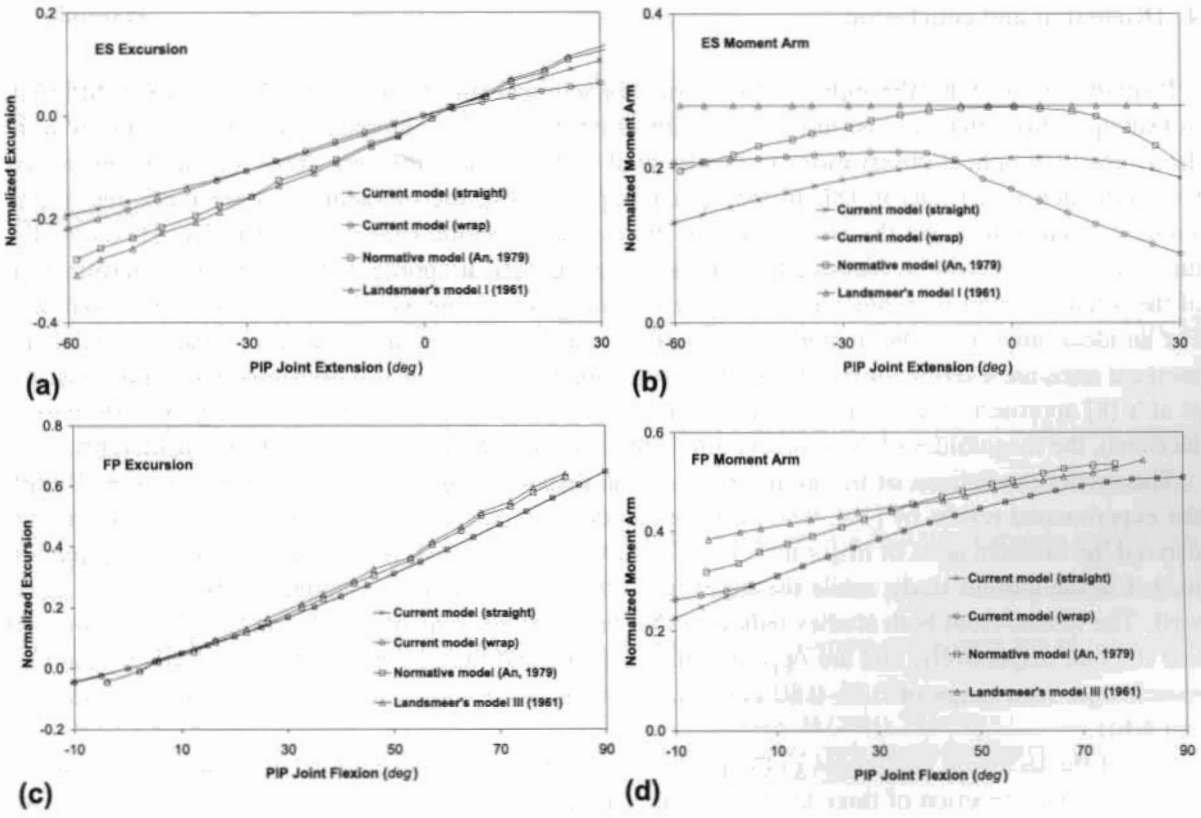

Fig. 5. The predicted muscle/tendon excursions and moment arms as a function of the PIP joint extension compared with those obtained using normative model [7] and Landmeer's model III [5,6]. (a and b) Excursions and moment arms of ES muscle (it is equivalent to EC/EI), respectively. (c and d) Excursions and moment arms of FP muscle, respectively. Both excursions and moment arms have been normalized by dividing with the middle phalanx length (i.e., O_2O_3 as shown in Fig. 1).

In Fig. 5, the excursions and moment arms of the ES and FP muscles for the PIP joint extension/flexion predicted using the current models are compared with those using the normative model [7] and Landsmeer's models [5,6]. In order to investigate the effects of considering realistic geometry of the bony section in the current model, we have compared the simulations considering the muscle/tendon wrapping over the surface of the bony sections (labeled as wrap in the figures) and those considering the muscle/tendon as a straight line between the attachment sites on the bone (labeled as straight in the figures). The muscle excursions and moment arms in these figures have been normalized by dividing by the middle phalanx length (i.e., O_2O_3 as shown in Fig. 1), which is estimated to 20.77 mm using Eq. (1). The model predictions on the ES (it is considered to be equivalent to EC/EI) muscle excursion and moment arms for the PIP joint extension are comparable with the normative model [7] and Landsmeer's model I [5] (Fig. 5(a) and (b)). The muscle excursions calculated by all three models agree well, while the muscle moment arms obtained by these different approaches differ considerably. The moment arm calculated using the Landsmeer's model is constant, while those obtained using normative and current models vary as a function of the PIP joint angle. For the FP muscle in response to the PIP joint flexion, the predicted excursion agrees well with those obtained using Landsmeer's model and normative models (Fig. 5(c)), while the predicted muscle moment arm is slightly smaller than those obtained using the other two models (Fig. 5(d)).

4. Discussion and conclusion

It should be noted that the approach to measure the moment arm in Fowler et al.'s [9] study is different, in principle, from that applied in [8] and in the current study. The moment arms of the m